TATA Box-Binding Protein–Associated Factor 12 Is Important for RAS-Induced Transformation Properties of Colorectal Cancer Cells

Angeliki Voulgari,[1] Stella Voskou,[1] Làszlò Tora,[2] Irwin Davidson,[2] Takehiko Sasazuki,[3] Senji Shirasawa,[4] and Alexander Pintzas[1]

[1]Laboratory of Signal Mediated Gene Expression, Institute of Biological Research and Biotechnology, National Hellenic Research Foundation, Athens, Greece; [2]Institut de Génétique et de Biologie Moléculaire et Cellulaire, Centre National de la Recherche Scientifique/Institut National de la Sante et de la Recherche Medicale/ULP, CU de Strasbourg, France; [3]Department of Pathology, International Medical Center of Japan, Tokyo, Japan; and [4]Department of Cell Biology, Faculty of Medicine, Fukuoka University, Fukuoka, Japan

Abstract

Activating mutations in the *RAS* proto-oncogene result in constant stimulation of its downstream pathways, further leading to tumorigenesis. Transcription factor IID (TFIID) can be regulated by cellular signals to specifically alter transcription of particular subsets of genes. To investigate potential links between the regulation of TFIID function and the RAS-induced carcinogenesis, we monitored the expression of the TATA box-binding protein and its associated factors (TAF) in human colon carcinoma cells. We primarily identified TAF12 levels as being up-regulated in cell lines bearing natural RAS mutations or stably overexpressing a mutated RAS isoform via a mitogen-activated protein kinase/extracellular signal-regulated kinase kinase–dependent pathway. We further showed by electrophoretic mobility shift assays and chromatin immunoprecipitation that the ETS1 protein was interacting with an ETS-binding site on the *TAF12* promoter and was regulating *TAF12* expression. The binding was enhanced in extracts from oncogenic RAS-transformed cells, pointing to a role in the RAS-mediated regulation of *TAF12* expression. Reduction of TAF12 levels by small interfering RNA treatment induced a destabilization of the TFIID complex, enhanced E-cadherin mRNA and protein levels, and reduced migration and adhesion properties of RAS-transformed cells with epithelial to mesenchymal transition. Overall, our study indicates the importance of TAF12 in the process of RAS-induced transformation properties of human colon cells and epithelial to mesenchymal transition, most notably those related to increased motility, by regulating specifically expression of genes such as *E-cadherin*.

(Mol Cancer Res 2008;6(6):1071–83)

Introduction

Colorectal cancer develops through a multistage process known as the adenoma-carcinoma sequence, which drives normal mucosa to invasive carcinoma through early and advanced adenomas. Each step of the sequence occurs in parallel with the stepwise accumulation of genetic alterations that gradually result in tumor development and progression (1).

RAS is a monomeric, membrane-localized G protein. In mammalian cells, there are three related but distinct *RAS* genes, encoding for Kirsten (*Ki-RAS*), neuroblastoma (*N-RAS*), and Harvey (*Ha-RAS*) RAS proteins. All three proteins have been related to specific types of cancer because activating mutations result in constitutive signaling (2). Activated RAS mediates its biological activity via Raf/mitogen-activated protein kinase/extracellular signal-regulated kinase (ERK) kinase (MEK)/ERK kinase pathways that in return regulate transcription factors, such as the AP-1 and ETS families, to subsequently induce genes such as *c-FOS* (3, 4).

Interestingly, the incidence of *K-RAS* mutations in colorectal cancer reaches 50%. Deletion of the activated *RAS* allele suppresses the malignant phenotype in the human colon cancer cell lines DLD-1 and HCT116 (5). Mutant Ha-RAS has a low incidence in colorectal tumors but shows the highest transformation potential among the RAS proteins in NIH3T3 (6) and colon epithelial cells (7). In Caco-2 cells, it induces an epithelial to mesenchymal transition (EMT), which results in enhanced tumorigenicity and changes in cell morphology (7). EMT induces dramatic changes to the cells, which switch from a polarized epithelial to a highly motile mesenchymal phenotype related to cancer progression, invasion, and metastasis (8, 9).

Transcription factor IID (TFIID) is a large multiprotein complex composed of the TATA box-binding protein (TBP) and several TBP-associated factors (TAF). TBP and TAFs are highly regulated (10, 11). Interestingly, rather than affecting

Received 8/9/07; revised 1/28/08; accepted 4/28/08.
Grant support: EU research grants LSHG-CT-2004-502950 and HPRN-CT 00504228 (A. Pintzas) and EU research grant LSHG-CT-2004-502950 (A. Voulgari).
The costs of publication of this article were defrayed in part by the payment of page charges. This article must therefore be hereby marked *advertisement* in accordance with 18 U.S.C. Section 1734 solely to indicate this fact.
Requests for reprints: Alexander Pintzas, Laboratory of Signal Mediated Gene Expression, Institute of Biological Research and Biotechnology, National Hellenic Research Foundation, 48 Vasileos Konstantinou Avenue, Athens 11635, Greece. Phone: 30-210-7273753; Fax: 30-210-7273755. E-mail: apint@eie.gr

doi:10.1158/1541-7786.MCR-07-0375

transcription globally, modified forms of TFIID selectively alter specific transcription networks. For instance, in cooperation with c-Jun, TAF4b can drive tissue-specific programs of gene expression (12), whereas other TAFs have been involved in particular phases of the cell cycle (13). Notably, *TBP* is up-regulated by a RAS-stimulated signaling pathway (14) potentially via an ETS protein-binding site on *TBP* promoter (15); (16) and contributes to cellular transformation in colon carcinoma cell lines (17).

TAF4 and TAF12 form a heterodimer important in the TFIID assembly (18). The TAF4 family also comprises the tissue-specific TAF4b, a substoichiometric subunit of TFIID able to heterodimerize with TAF12. Human TAF4 interacts with transcription factors involved in cell signaling (19, 20). Inactivation of TAF4 in mouse fibroblasts activates the transforming growth factor β signaling pathway (21). On the other hand, TAF12 has been linked to transcriptional activation, particularly through a direct interaction with ATF7, known to heterodimerize with Jun/Fos transcription factors (22). However, little is known about the involvement of TAF12 in cell proliferation.

We investigated potential changes in the expression of TBP and TAFs during carcinogenesis via mutated RAS in human colon carcinoma cell lines. Herein, evidence is presented that *TAF12* is transcriptionally up-regulated in cell lines expressing mutant RAS to actively participate in cellular transformation by affecting *E-cadherin* expression.

Results

Levels of TAF12 Are Enhanced in Human Colon Carcinoma Cells and in Cell Lines Expressing Mutant Oncogenic RAS *Isoforms*

We began by testing whether the multistep colorectal carcinogenesis process, driving cells from adenoma to adenocarcinoma, could affect the levels of TFIID components. For that, nuclear extracts from several cell lines were prepared and analyzed by Western blot. Among the tested proteins, TBP, TAF4, TAF4b, and TAF12 levels varied compared with β-actin (Fig. 1A; data not shown). Interestingly, TAF12 expression was enhanced in cells containing an activating mutation of Ki-RAS (8-fold in HCT116 and DLD-1 cells and 6.5-fold in SW620 compared with Caco-2 cells). In parallel, TAF4 and TBP levels presented a smaller but significant increase in SW620 and HCT116, whereas TAF4b levels presented changes unrelated to RAS.

To test the hypothesis of a TAF12 RAS-dependent expression, we used Caco-2 cell lines stably overexpressing a mutated, constantly active form of Ki-RAS and Ha-RAS. Caco-2 cells carrying the Ki-RASV12 mutation are named Caco-K (clones 6 and 15) and those carrying the Ha-RASV12 are named Caco-H (clones 1 and 2). Enhanced levels of Ki-RAS and Ha-RAS as well as levels of phosphorylated ERK corresponding to a MEK activity were confirmed by Western blot (Fig. 1B). Studies on mRNA levels also confirmed the specific overexpression of the *RAS* isoforms in the corresponding cell line (data not shown). Interestingly, levels of TAF12 were increased by 3-fold in extracts from Caco-H cells compared with Caco-2 (Fig. 1B, *lanes 1-3*), whereas in Caco-K15 cells an increase of 2.7-fold was observed (*lanes 4* and *5*). Smaller variations were observed for TAF4 and TBP levels. In extracts from HKE3 cell line, derived from HCT116 cells after disruption of mutated Ki-RAS allele, TAF12 expression was decreased (Fig. 1C). Notably, TBP expression was also decreased in HKE3 cells. For the rest of the study, we focused on the RAS-dependent regulation of TAF12 in Caco-H cells because the up-regulation of TAF12 was the strongest. In parallel, we were particularly interested in a potential role of TAF12 in the EMT, observed specifically in the Caco-H cells.

A microarray analysis conducted using the RZPD Oncochip showed a 2.9-fold up-regulation of *TAF12* mRNA in Caco-H cells, suggesting a mechanism of transcriptional regulation (7). To validate this, we used both standard reverse transcription-PCR and real-time PCR (Fig. 1D). Compared with Caco-2 cells, *TAF12* mRNA levels were increased by 5-fold in Caco-H cells (*lanes 2* and *3*) and to a lesser extent in Caco-K15 cells (*lane 5*), whereas no significant up-regulation was observed for the Caco-K6 clone, possibly due to low MEK activity. In parallel, a 5-fold induction of *TAF12* mRNA was found in the SW620 cell line (*lane 6*), which had also high levels of TAF12 protein (Fig. 1A, *lane 2*).

To identify the mechanism implicated in *TAF12* regulation by RAS, we used the UO126 inhibitor to block the Raf/MEK/mitogen-activated protein kinase pathway. Treatment of Caco-2 and Caco-H1 cells with UO126 in a rich medium resulted in a partial inhibition of the MEK activity but had little effect on TAF12 expression (Fig. 1E, *lanes 1* to *2* and *lanes 3* to *4*; 61% and 42% inhibition of phosphorylated ERK, respectively). After serum starvation, levels of phosphorylated ERK were low in Caco-2 but not in Caco-H cells. Under these conditions, the UO126 inhibitor did not further affect the MEK activity in Caco-2 cells (*lanes 5* and *6*) but had a strong inhibitory effect (75%) on Caco-H cells (*lane 7*). In these cells, TAF12 showed a reduction of 60% (*lane 8*), suggesting that its expression is regulated via a MEK-dependent mechanism.

Together, those results show that TAF12 levels vary between different colorectal adenocarcinoma cell lines. Notably, TAF12 is transcriptionally enhanced via a MEK-dependent mechanism in the presence of the mutated Ha-RAS protein and, in a lesser extent, Ki-RAS protein stably overexpressed in Caco-2 cells.

The TAF12 *Promoter Contains a RAS-Responsive Consensus ETS-Binding Site*

To dissect the mechanism by which RAS affects the transcription of *TAF12*, we analyzed the proximal promoter region of *TAF12* for oncogene-responsive transcription factor binding sites using MatInspector and Transfac. Among several putative binding sites, a sequence matching the consensus recognition site for the ETS family DNA-binding proteins was identified from −21 to −13. Sequence alignment in Fig. 2A shows that both the *TBP* and *TAF12* promoter ETS-binding sites were similar to the optimum consensus recognition site for the endogenous human ETS1 protein on the *ETS1.3* promoter (23). Moreover, sequence comparison of the human, mouse, and rat *TAF12* proximal promoter revealed a high degree of conservation (Fig. 2B), underlying an important role in *TAF12* transcriptional regulation. To test the functionality of this site, we did gel shift assays using nuclear extracts from H1 cells and

a set of two probes corresponding to the *TAF12* promoter putative ETS-binding site (ETST12) and the consensus ETS1-binding site on the *ETS1.3* promoter (ETS1.3). The presence of the ETST12 probe induced the specific binding of a protein complex (Fig. 2C, *lane 5*). The interaction was abolished by the addition of an excess of nonradiolabeled ETST12 probe (*lane 6*) but not by that of a nonspecific competitor probe containing the AP-1–binding site of the *vimentin* promoter (*lane 8*). The binding was specific because the ETST12mut probe bearing a point mutation in the central core of the *TAF12* promoter ETS-binding site failed to form the complex (*lane 10*). Moreover, ETST12 and ETS1.3 probes were in competition for protein binding when present together (*lane 7*), suggesting that similar protein complexes could interact with both DNA sequences. To determine a potential role of the ETS-binding site in the RAS-dependent regulation of *TAF12*, we monitored its occupancy in the presence of different protein extracts. As shown in Fig. 2D, the DNA-binding activity detected in Caco-H1 was stronger than that observed in Caco-2 extracts, in agreement with increased *TAF12* mRNA levels (Fig. 1D).

Those results show that an ETS-binding site found on the *TAF12* promoter is specifically recognized by a protein complex. Its occupancy is increased in cells containing the mutated form of Ha-RAS, pointing to a specific role in TAF12 up-regulation.

The ETS1 Protein Binds to the TAF12 Promoter to Regulate the TAF12 Gene Expression in Caco-H Cells

To identify whether the ETS1 protein was a member of the protein complex binding the ETS site on *TAF12* promoter, we first analyzed the levels of ETS1 protein in the *RAS*-transformed

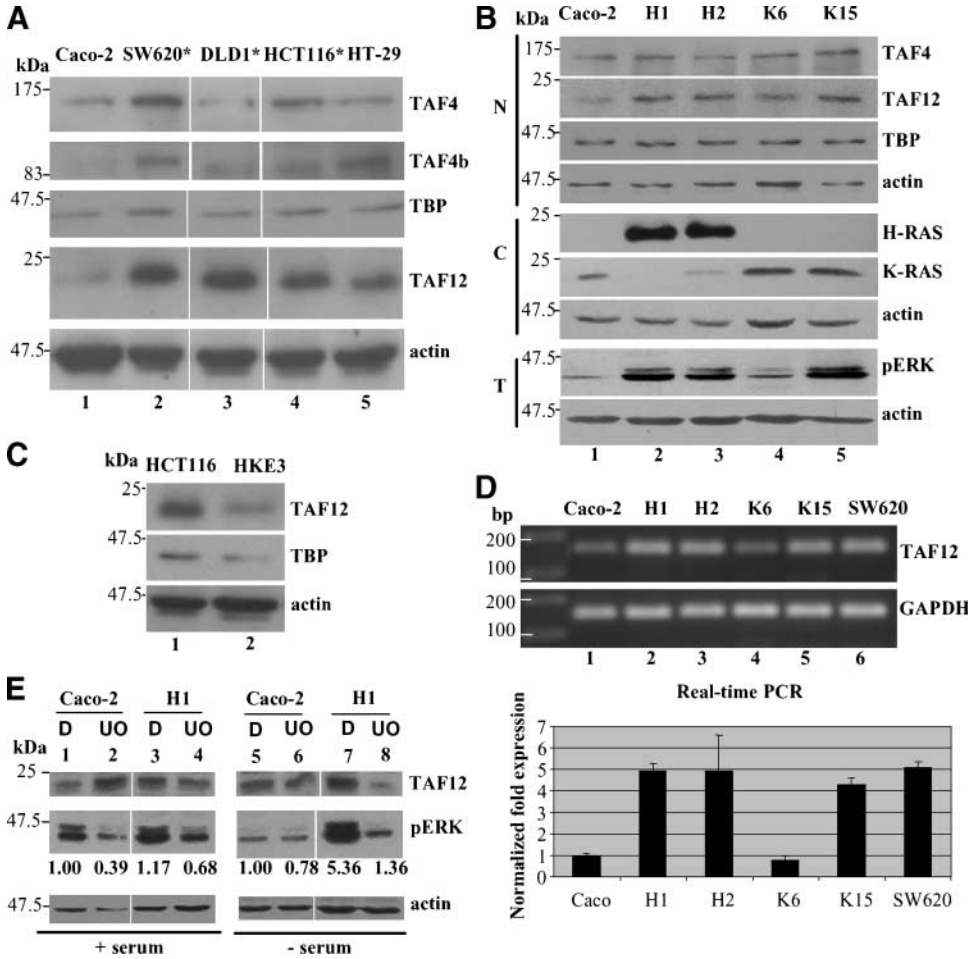

FIGURE 1. TBP and several TAFs are differentially expressed in human colon carcinoma cell lines and cell lines carrying RAS mutations. **A.** Total extracts from the indicated colorectal cell lines were subjected to Western blot analysis. Cell lines bearing Ki-RAS mutations are noted with an asterisk. Size of the protein markers is expressed in kDa. Lanes that were not contiguous in the gel are marked by a dividing line. **B** and **C.** Nuclear (*N*), cytoplasmic (*C*), or total (*T*) extracts from cells overexpressing mutant RAS [Caco-2→Caco-H (H1-H2) and Caco-K (K6-K15)] or cells where the mutant RAS allele was inactivated (HCT116→HKE3) were used for Western blot analysis as indicated. **D.** cDNA from indicated cell lines was subjected to PCR and real-time PCR. DNA markers are expressed in base pairs (*bp*). For real-time PCR, TAF12 expression values were normalized to GAPDH and adjusted to the Caco-2 cell expression assigned as 1. **E.** Caco-2 and Caco-H1 were treated with DMSO (*D*) or the MEK inhibitor UO126 (*UO*). Cells were cultured in the presence (+) or absence (–) of serum. Total extracts were used for Western blot analysis. Intensity of the phosphorylated ERK (*pERK*) corresponding band was measured, adjusted to the DMSO-treated Caco-2 cells for each condition, and depicted below the corresponding blot. Nonadjacent lanes were combined from a single electrophoresis gel.

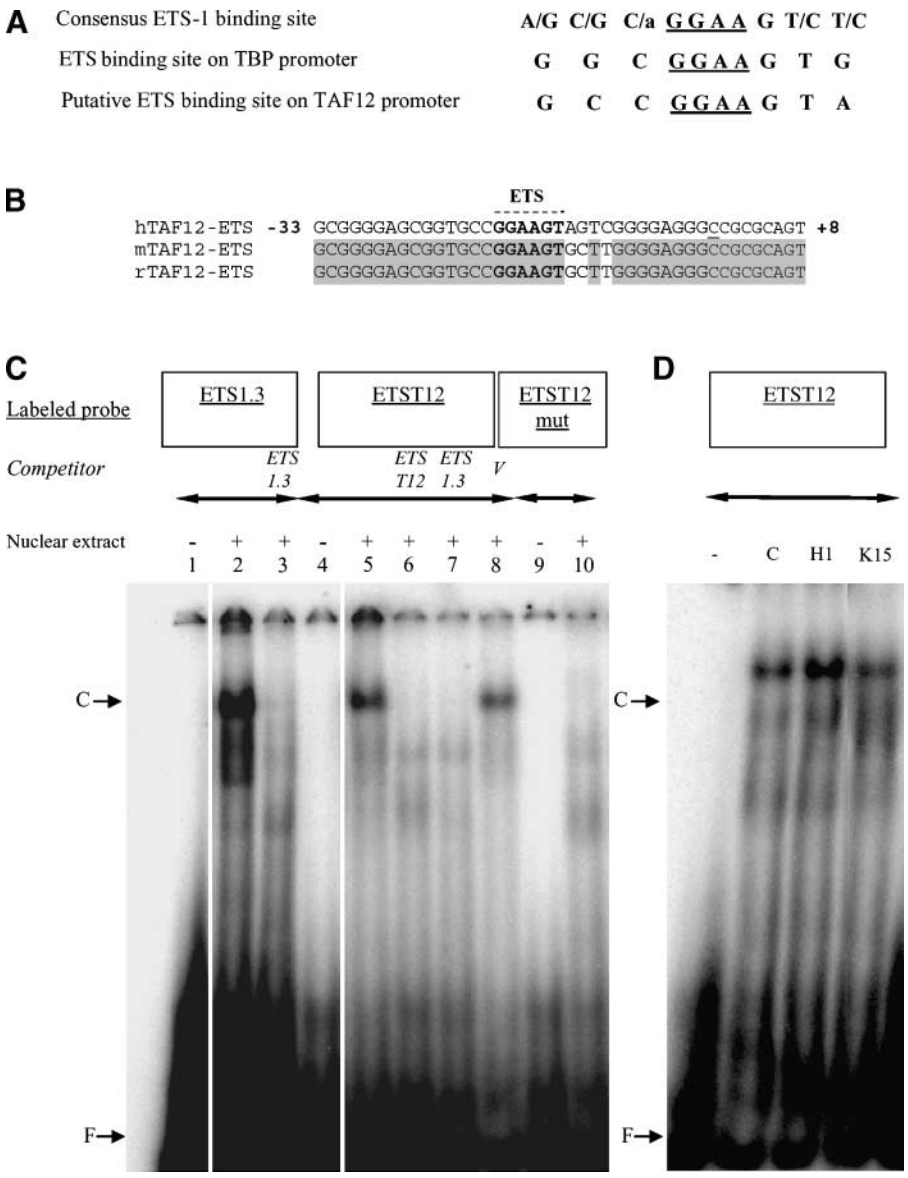

FIGURE 2. Identification and analysis of a RAS-responsive ETS-binding site present on the promoter of TAF12. **A.** Sequence alignment of the consensus ETS1-binding site, the ETS-binding site of the *TBP* promoter, and the putative ETS-binding site of the *TAF12* promoter. The central core of the site is underlined. **B.** Sequence comparison of the specific *TAF12* promoter region between human (*hTAF12*), mouse (*mTAF12*), and rat (*rTAF12*). Shaded regions indicate perfect homology with human sequence. ETS sequence is indicated in bold. Positions are indicated in base pairs according to the transcription initiation site, which is underlined. **C.** Gel shift analysis was done using labeled probes (*underlined*) containing the ETS-binding site. Probes were incubated in the presence (+) or absence (−) of Caco-H1 cell nuclear extracts. For competition experiments (in *italic*), excess of the indicated unlabeled probe was added. Vimentin AP-1–binding site (*V*) was used as a nonspecific competitor. Free probe (*F*) and ETS site-specific protein complexes (*C*) are indicated. Lanes that were not contiguous on the same gel are marked by a space. **D.** Gel shift analysis was done with ETST12-labeled probe in the absence of proteins (−) or in the presence of nuclear proteins from Caco-2 (*C*), Caco-H1 (*H1*), and Caco-K15 (*K15*) cell lines.

clones. As seen in Fig. 3A (*lanes 2* and *3*), expression of ETS1 was found to be enhanced in Caco-H cells, where the occupancy of the ETS site was the highest in electrophoretic mobility shift assay (Fig. 2D). In parallel, the phosphorylated form of the ternary complex factor member ELK1 was also increased. When electrophoretic mobility shift assay was done in the presence of an antibody directed against ETS1, a small decrease of the signal intensity and the appearance of a weak shifted protein complex were observed (Fig. 3B, compare *lanes 1* and *2*), suggesting a binding of the ETS1 protein on the ETS site of the *TAF12* promoter. To verify this hypothesis *in vivo*, chromatin immunoprecipitation (ChIP) of cross-linked chromatin from Caco-H1 cells was done. Immunoprecipitation was followed by PCR with primers encompassing the ETS site of the *TAF12* promoter. As seen in Fig. 3C, *a*, the promoter region containing the ETS site was efficiently amplified from chromatin precipitated with an antibody recognizing the ETS1 protein (*lane 4*), whereas an antibody recognizing the ELK1 protein failed to precipitate this fragment (*lane 5*). Dilutions of the input chromatin were used as a positive control (*lanes 1-3*),

whereas as a negative control a reaction done in the absence of any antibody was done (*lane 6*). To further show an *in vivo* role of the ETS1 protein binding in the Ha-RAS–induced *TAF12* up-regulation, ChIP was done in the presence of an anti-ETS1 antibody and extracts from Caco-2, Caco-H1, and Caco-K15 cell lines. As seen in Fig. 3C, *b*, more ETS1 binding on *TAF12* promoter was observed in Caco-H1 (*lane 5*) compared with Caco-2 and Caco-K15 cells (*lanes 4* and *6*). As a positive control for ChIP, an antibody directed against acetylated histone H3 immunoprecipitated the ETS site on *TAF12* promoter (*lane 8*). A second set of primers encompassing the ETS site of *TAF12* promoter produced identical results (data not shown).

To further show the role of the ETS1 protein in *TAF12* regulation, short interfering RNA (siRNA)-mediated knockdown of the ETS1 protein was done. As seen in Fig. 3D, *a*, 48 h after transfection of Caco-H1 cells with the ETS1 siRNA, ETS1 was efficiently knocked down (*lane 3*). No effect was observed for the mock control (*lane 1*) and the nontargeting control siRNA (*lane 2*). RNA extracted from transfected cells was reverse transcribed and used to analyze the expression of both *ETS1* and *TAF12*. Real-time PCR in Fig. 3D, *b* confirmed an important, 5-fold decrease of the *ETS1* mRNA in ETS1 siRNA-treated cells and a smaller but significant decrease of the *TAF12* mRNA.

Together, those results show that an ETS-binding site upstream of the transcription initiation site of *TAF12* binds specifically, *in vitro* and *in vivo*, the human ETS1 protein. Binding to this site is higher in Caco-H1 cells, suggesting a role in the RAS-mediated *TAF12* promoter regulation. The knockdown of ETS1 is accompanied by a decrease of *TAF12,* pointing to a physiologic role of ETS1 in *TAF12* regulation.

Reduction of TAF12 Destabilizes the TFIID and Alters the Morphology of Caco-H Cells

To assess the cellular role(s) of TAF12, siRNA-mediated knockdown of the protein was done. As seen in Fig. 4A, 48 h after transfection of the cells by a synthetic siRNA duplex targeting *TAF12* mRNA (*lane 3*), a reduction of intracellular TAF12 protein levels was observed compared with the control conditions (*lanes 1* and *2*). As expected, knockdown of TAF12 was paralleled by a decrease in levels of other TAFs, probably corresponding to loss of protein stability (Fig. 4B, *lanes 1* and *3*; data not shown). For instance, TAF4b was slightly decreased; TBP exhibited a moderate effect, whereas TAF10 was highly affected. Despite the effects due to down-regulation of TAF12, cells containing reduced TAF12 grew normally and only exhibited an apoptotic-related decrease in cell number corresponding to 20% and 25% of the control cells (48 and 72 h after transfection, respectively). Notably, TAF12 siRNA but not the control cells exhibited a particular change in cell morphology resulting in the appearance of long processes emanating from the cell body (Fig. 4C, *top*, siTAF12, *black arrows*). Processes were visible both under a light microscope (*top*) and after cell staining with an antibody recognizing the β-actin protein (*bottom*).

The above experiments suggest that a reduction of TAF12 by siRNA is not lethal but induces a decrease in protein levels of other TAFs and modifies the phenotype of transformed cells.

TAF12 Expression Alteration Modulates the Migration and Adhesion Properties of Caco-H Cells

To identify a specific role of TAF12 in the RAS-induced carcinogenesis, we analyzed cell properties that were known to be modified by activated Ha-RAS or during EMT, such as adhesion and migration (Fig. 5). Interestingly, treatment of cells with TAF12 siRNA significantly blocked migration by 40% compared with the control siRNA-treated cells and by 60% compared with the nontreated cells. As a control, only 1% of the parental cell line Caco-2 showed a migrating capacity compared with its Ha-RAS–transformed counterpart Caco-H1, which has an EMT. In parallel, in cell adhesion assays, the

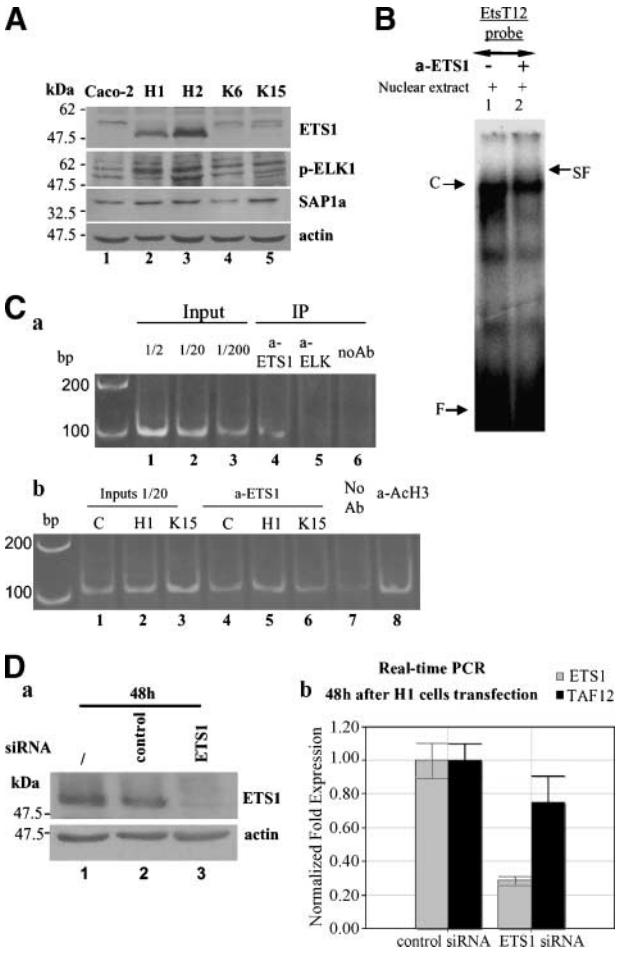

FIGURE 3. The ETS1 protein binds and regulates the TAF12 promoter. **A.** Nuclear extracts from different cell lines were subjected to Western blot analysis with the indicated antibodies. Size of the protein markers is expressed in kDa. **B.** Gel shift analysis was done in the presence of Caco-H1 cells nuclear extracts and in the presence (+) or absence (–) of an anti-ETS1 antibody. Free probe (*F*), ETS site-specific protein complexes (*C*), and supershifted protein complexes (*SF*) are indicated. **C.** ChIP of the TAF12 promoter was done with *in vivo* cross-linked chromatin extracted from Caco-H1 (*a*) or Caco-2, Caco-H1, and Caco-K15 cells (*b*). Immunoprecipitation (*IP*) was done with the indicated antibodies or in the absence of antibody (*no Ab*). The precipitated DNA fragments were amplified by PCR. **D.** a, total proteins from untreated (*/*) Caco-H1 cells and cells treated with control or ETS1 siRNA for 48 h were extracted and analyzed by Western blot. b, real-time PCR analysis of *ETS1* and *TAF12* cDNA levels in Caco-H1 cells treated with control or ETS1 siRNA for 48 h. Data were normalized to GAPDH and expressed as a relative expression of treated versus untreated cells.

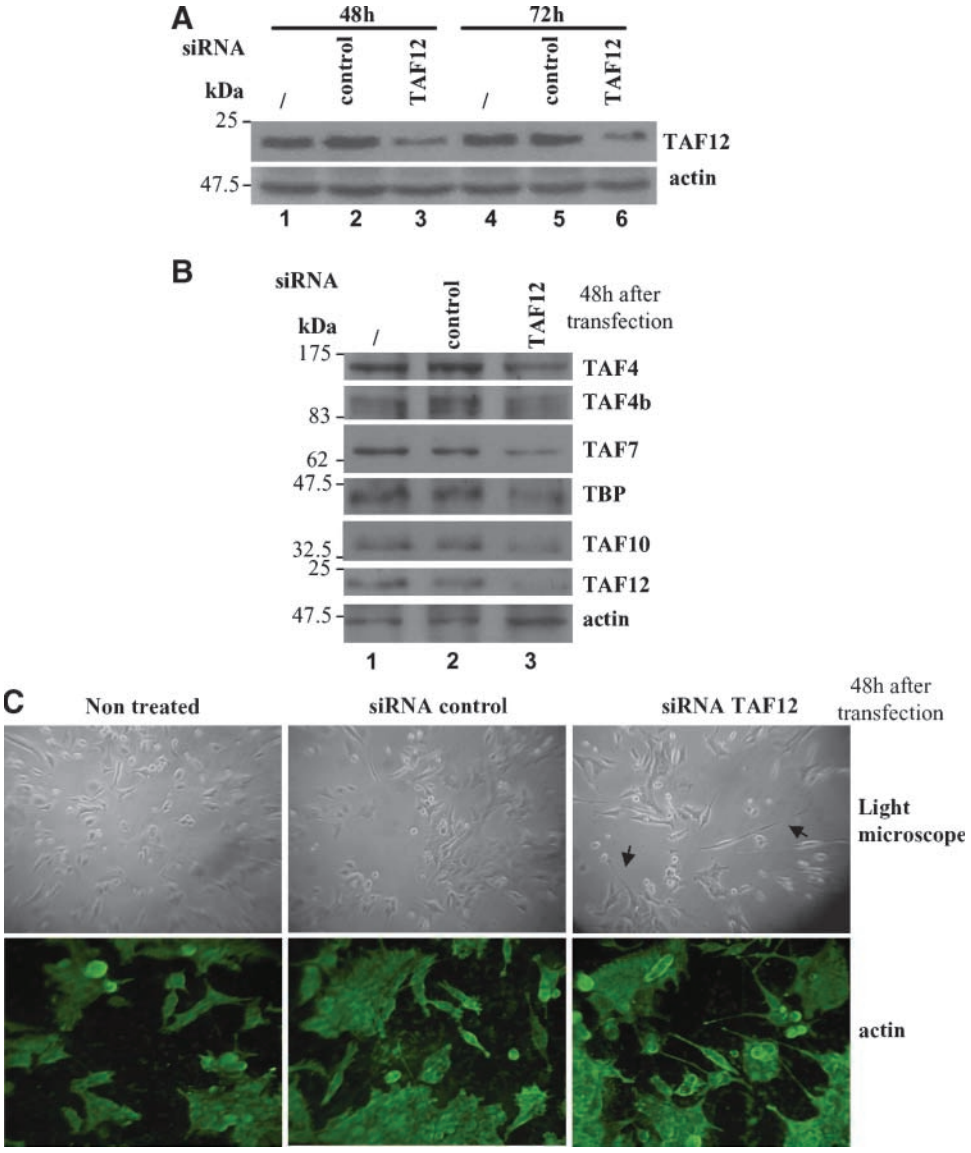

FIGURE 4. Knockdown of TAF12 in Caco-H1 cells by siRNA. **A.** Total proteins from untreated (/) Caco-H1 cells and cells treated with control or TAF12 siRNA for 48 and 72 h were extracted and analyzed by Western blot. **B.** Nuclear extracts from siRNA-treated cells (48 h) were analyzed by Western blot as indicated. **C.** Top, live cell images of control or siRNA-treated cells using a light microscope. Black arrow, long cellular structures are observed in TAF12 siRNA-treated cells. Bottom, indirect immunofluorescence of treated cells was done using an anti-actin antibody. Magnification, ×20.

cellular capacity to form complexes between the cytoskeleton and an extracellular matrix component, such as fibronectin, was diminished by 30% in cells treated with the TAF12 siRNA (Fig. 5B). Again, the Caco-2 cell line showed a restricted adhesive capacity compared with Caco-H1.

Together, those results show that the reduction of TAF12 is accompanied by a reduction of the adhesion and migration properties of mutated Ha-RAS–transformed cells. Further comparison of Caco-2 and Caco-H shows that mutated Ha-RAS transformation and consequent EMT dramatically increases these properties.

E-Cadherin *mRNA and Protein Levels Are Increased following TAF12 Reduction*

In an attempt to identify TAF12 target genes related to RAS transformation and EMT, reverse transcription-PCR analysis was used to monitor changes in the expression of several genes in TAF12 knockdown cells (Fig. 6A; data not shown). The genes tested code for different families of molecules such as cell surface receptors (*E-cadherin* and *Integrin A6*), intermediate filaments (*vimentin*), or transcription factors (*TBP*). Interestingly, most of the genes tested showed no difference in their expression after TAF12 reduction. Notably, only the *E-cadherin* mRNA quantity was altered, exhibiting an increase paralleled to the decrease of *TAF12* mRNA. To quantify the effect of TAF12 on *E-cadherin* expression, we analyzed the expression of both genes using real-time PCR 48 h after transfection of Caco-H cells with TAF12 siRNA. As shown in the graph represented in Fig. 6A, a 2.5-fold reduction of *TAF12* mRNA resulted in a 2.7-fold increase of *E-cadherin* mRNA levels. This increase was also confirmed at the protein level (Fig. 6B, *lane 3*). To test whether the morphologic changes observed in TAF12 knockdown cells (Fig. 4C) were associated to the reexpression of E-cadherin, we did immunofluorescence experiments (Fig. 6C). In siRNA-transfected cells (*bottom*), E-cadherin–associated signal (*red*) was covering the

entire cell surface as well as the characteristic cell extensions. On the contrary, in nontransfected cells (*top*), E-cadherin signal was weak and diffuse. To confirm the effect of TAF12 reduction on *E-cadherin*, we used TAF12 siRNA in the HCT116 cell line, which naturally has high levels of TAF12 (Fig. 1A). Reverse transcription of total RNA followed by real-time PCR showed that a 2.5-fold reduction of *TAF12* was accompanied by a 1.3-fold increase of *E-cadherin* (Fig. 6D).

Those results show that TAF12 reduction has no effect on the overall cellular transcription. On the contrary, they underline a specific role of TAF12 down-regulation on E-cadherin up-regulation both at the mRNA and protein levels.

TAF12 *and* E-Cadherin *Follow an Inverse Pattern of Expression in Colorectal Cell Lines and during EMT*

To examine the relation between *TAF12* and *E-cadherin* in more physiologic conditions, we analyzed the expression of E-cadherin in the RAS-transformed cells (Fig. 7A). In those conditions, both mRNA (Fig. 7A, *a*) and protein levels (Fig. 7A, *b*) of E-cadherin were dramatically reduced in Caco-H cells where TAF12 levels were found to be enhanced.

We next examined the E-cadherin levels in total extracts from colorectal cell lines. The Western blot in Fig. 7B, *a* showed that each cell line contained different amounts of E-cadherin: Caco-2, HT-29, and DLD-1 cells (*lanes 1-3*) had an important amount of protein, HCT116 and SW620 cells had barely detectable amounts (*lanes 4* and *5*), whereas the protein was no more detectable in Caco-H cells (*lane 6*). Interestingly enough, TAF12 expression was inversely proportional to that of E-cadherin. In addition, TAF12 increase was accompanied by an enhancement of the ETS1 expression, in agreement with an ETS1-dependent *TAF12* regulation. As E-cadherin is an EMT marker, we also examined the levels of the second EMT marker, vimentin. As seen in Fig. 7B, *a*, vimentin expression was inversely proportional to that of E-cadherin, pointing on the existence of distinct stages of EMT in the panel of colorectal cell lines examined. To verify the parallel change in the expression of *E-cadherin* and *TAF12* in this transition, real-time PCR was done on cDNA synthesized from Caco-2 and HCT116 cells. As seen in Fig. 7B, *b*, a 2.2-fold up-regulation of *TAF12* mRNA in HCT116 cells was accompanied by a 30-fold reduction of the *E-cadherin* gene expression.

Finally, we examined by real-time PCR the expression pattern of *E-cadherin* in the HKE3 cell line, created by knockout of the naturally mutated Ki-RAS allele in HCT116 cells, where TAF12 expression was found to be altered (Fig. 1C). Interestingly, *E-cadherin* mRNA increased by 1.3-fold in HKE3 cells, whereas *TAF12* mRNA was comparably decreased (Fig. 7C).

Together, those results show that TAF12 and E-cadherin display a common pattern of expression in established colorectal cell lines. This agrees with a role of TAF12 on *E-cadherin* regulation in colorectal cancer and EMT.

Discussion

TAF12 Expression Is Altered during RAS-Induced Tumorigenesis and EMT

We have examined the expression pattern of TBP and TAFs in human epithelial colorectal adenoma Caco-2 cells stably expressing mutant, constantly activated forms of Ha-RAS and Ki-RAS. Herein, we provide evidence that TAF12 is up-regulated via oncogenic RAS signaling, mediated in part by the MEK pathway. In our knowledge, TAF12 is the first example of a TAF regulated by the RAS transforming function. Nevertheless, the identification of *TBP* as a RAS target gene supports the idea that the general transcription machinery activity could control transcription initiation in carcinogenesis events (14, 17).

We have previously shown that mutated Ha-RAS and Ki-RAS modulate specifically or commonly the expression of a large panel of genes (7). In our hands, up-regulation of *TAF12* was common to both RAS-mutated isoforms, suggesting a central role of TAF12 in transformation by RAS. Nevertheless, the up-regulation of *TAF12* was significantly higher in Caco-H cells, which were clearly subjected to the EMT during the RAS transformation (7-24). Notably, as this particular cell alteration into mesenchyme is the critical event leading to invasiveness and metastasis in cancer, we have used the Caco-H cell line as a model for EMT and transition to final stages of colorectal cancer. In parallel, we have confirmed *TAF12* up-regulation during partial or complete EMT in established colorectal cell lines such as HCT116.

As a further support for the importance of TAF12 up-regulation in the development of cancer, we show that in the early-stage adenoma cells the expression of TAF12 is low

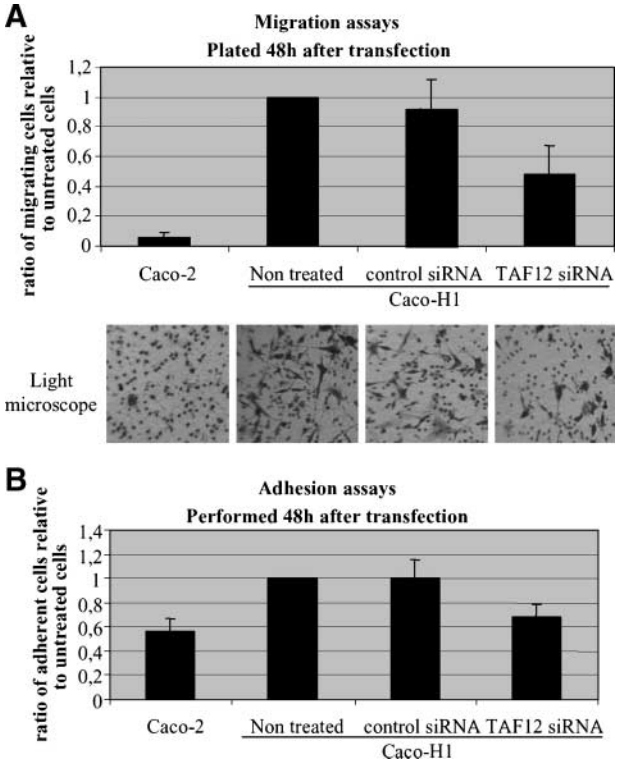

FIGURE 5. TAF12 down-regulation affects cell characteristics. Caco-2 and Caco-H1 cells treated with siRNA were analyzed for their ability to migrate in response to a chemotactic gradient (**A**) or to adhere on a fibronectin-coated substrate (**B**). Results were expressed as the ratio of cells capable to adhere or migrate relatively to the untreated cells assigned as 1. Photos correspond to a randomly selected field showing fixed and stained cells that have been able to migrate through the Transwell filter.

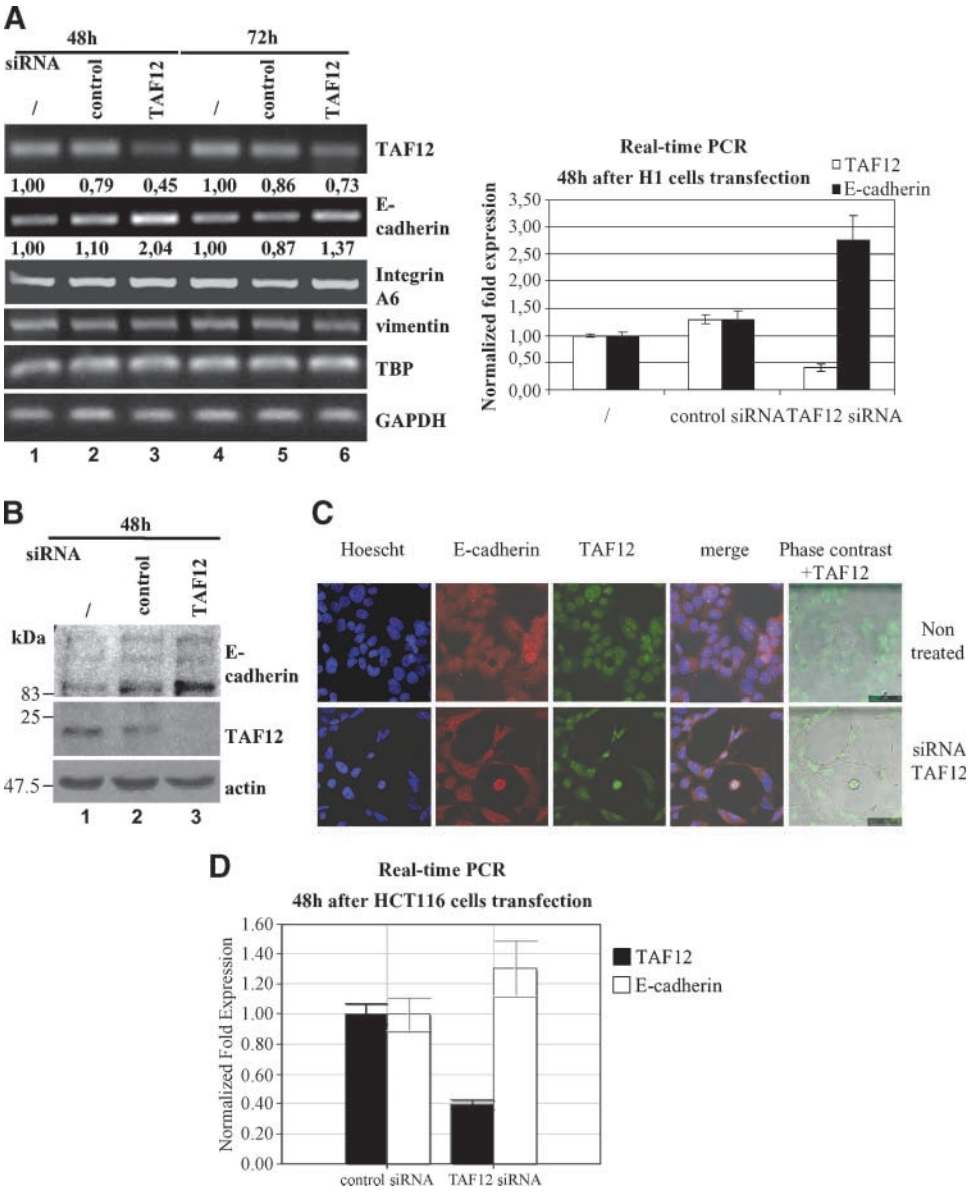

FIGURE 6. TAF12 down-regulation induces the expression of E-cadherin. **A.** cDNA from TAF12 siRNA-treated cells (48 and 72 h after transfection) was subjected to PCR analysis as indicated. Bands corresponding to TAF12 and E-cadherin cDNA were quantified, normalized to GAPDH expression, and expressed as a ratio to the expression of control cells. Real-time PCR analysis of *E-cadherin* and *TAF12* cDNA levels in Caco-H1 cells treated with control or TAF12 siRNA for 48 h. Data were normalized to GAPDH and expressed as a relative expression of treated versus untreated cells. **B.** Western blot analysis of total cell extracts treated with TAF12 siRNA for 48 h. **C.** Indirect immunofluorescence on fixed siRNA-treated cells was done using a TAF12 antibody (*green*) and an E-cadherin antibody (*red*) using a confocal microscope. Blue, nuclei were stained with Hoechst dye to label DNA. The same field was also examined in phase contrast. Merged images of the phase contrast and the TAF12 antibody signal are shown. **D.** Real-time PCR analysis of *TAF12* and *E-cadherin* cDNA levels in HCT116 cells treated with control or TAF12 siRNA for 48 h. Data were normalized to GAPDH and expressed as a relative expression of treated versus untreated cells.

compared with more advanced adenocarcinoma. We also show that TAF12 is transcriptionally regulated via a RAS-related mechanism. Accordingly, our initial study about the identification of RAS target genes by microarrays showed an up-regulation of both TBP and TAF12, which were at the time discriminated by the threshold applied (7), but further confirmed at the protein level. Notably, more TAF12 is monitored in DLD-1, SW620, and HCT116 cell lines, which bear an activating mutation of RAS. Nevertheless, the carcinoma HT-29 cell line containing wild-type RAS but mutant BRAF exhibits increased levels of TAF12 compared with the adenoma Caco-2 cells, suggesting the existence of a mechanism more probably related to the activation of the mitogen-activated protein kinase pathway and/or the activation of the ETS1 protein. Interestingly, a first study done in human colorectal tumors shows a small up-regulation of *TAF12* in a subset of the tissues tested, raising the possibility of TAF12 involvement in particular tumor characteristics (data not shown). Ongoing work on human tumor samples will potentially allow the identification of the *in vivo* role of TAF12.

RAS-Induced Transcriptional Regulation of TAF12 Is Mediated in Part by the Binding of the ETS1 Protein on TAF12 Promoter

The data obtained from the analysis of the *TAF12* promoter show that a putative ETS-binding site is functional in our cells. In parallel, we show by ChIP that the ETS1 protein binds to this site and is in part responsible for the RAS-mediated increase of *TAF12* mRNA. Moreover, knockdown of the ETS1 protein by siRNA is accompanied by a decrease in *TAF12* mRNA levels. Interestingly, the family of ETS transcription factors contains a large number of members that control the expression of genes

involved in cell proliferation, differentiation, and transformation (25). Notably, an ETS-binding site on the TBP promoter has been found to be involved in the RAS-mediated induction of the human promoter activity (14). Nevertheless, the results that we obtained in electrophoretic mobility shift assay done in the presence of an anti-ETS1 antibody suggest that the complex that binds the ETS site of *TAF12* promoter contains only a small proportion of the actual ETS1 protein. Like for *TBP*, other ETS family members may also be involved in *TAF12* regulation (26). In agreement, knockdown of the ETS1 protein affects only, in part, the expression of *TAF12*. This suggests that other ETS family members could replace ETS1 action on *TAF12* promoter or that, in the absence of the ETS1 protein, an ETS1-independent mechanism could be recruited to maintain levels of TAF12. Accordingly, our results show that TAF12 levels are reduced only when the MEK inhibitor is used in a low serum environment, possibly pointing to a more efficient inhibition of the MEK pathway in the absence of growth signals. Alternatively, this result could reflect the presence of a serum-dependent/MEK-independent mechanism acting on TAF12 expression. This suggests that, similarly to *TBP* promoter, at least one mechanism of regulation of TAF12 is acting independently of the ETS1 protein and the MEK/ERK pathway (14). Accordingly, TBP expression is altered by MEK inhibition in a low serum environment (14).

TAF12 Plays a Role in the EMT-Related Changes by Altering the Expression of E-Cadherin

E-cadherin, a molecule implicated in cell-cell adhesion, is silenced in Ha-RAS–transformed cells (Caco-H) with an

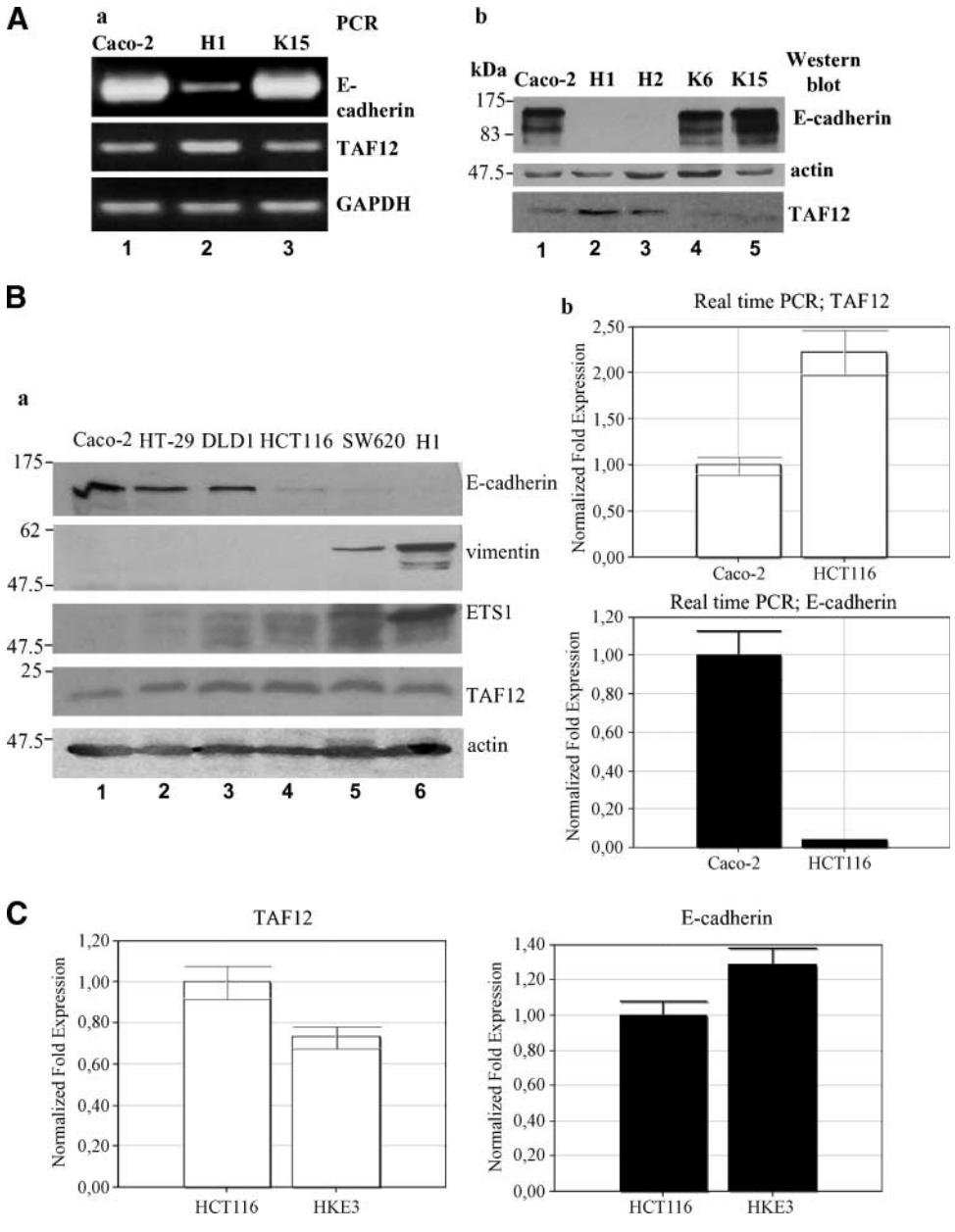

FIGURE 7. TAF12 and E-cadherin share a common expression pattern in colorectal cell lines. **A.** Total RNA (*a*) and total proteins (*b*) were extracted from Caco-2 and Caco-2 cells overexpressing the mutated Ha-RAS and Ki-RAS. Expression of E-cadherin and TAF12 was analyzed by reverse transcription-PCR and Western blot as indicated. Size of the protein markers is expressed in kDa. **B.** a, the same procedure was followed for extraction of total RNA and total protein extraction from several colorectal cell lines. b, quantification of *TAF12* and *E-cadherin* mRNA levels was done by reverse transcription followed by real-time PCR analysis. Values were normalized to GAPDH and adjusted to the Caco-2 cell expression assigned as 1. **C.** Real-time PCR analysis of TAF12 and E-cadherin mRNA levels after reverse transcription of total RNA extracted from HCT116 and HKE3 cells. Values were normalized to GAPDH and adjusted to the HCT116 cell expression assigned as 1.

EMT-related phenotype (27). We found that TAF12 reduction by siRNA produces a specific derepression of *E-cadherin* and subsequent inhibition of cell adhesion and migratory capacity both in Ha-RAS–transformed cells with EMT and in HCT116 cells with some EMT characteristics. Evidence from recent report suggests that TAF12 can act as a coactivator of the VDR activity (28). As *E-cadherin* expression is regulated by nuclear receptors and androgens as well as vitamin D itself (29), it is conceivable that TAF12 could have a role in this mechanism. Alternatively, TAF12 may interfere with the function of complexes that retain *E-cadherin* silenced, particularly those involved in histone modification and DNA methylation. This last hypothesis is supported by the fact that TAF12 is effective on *E-cadherin* expression preferentially in cells that have low basal (repressed) *E-cadherin* (data not shown). TAF12 regulation of *E-cadherin* can be critical for particular tumor properties because long-term repression of *E-cadherin* can induce EMT and its reexpression can suppress tumor invasion (30). This suggests that the full RAS cellular transformation needs particular changes in gene expression, potentially achieved by overexpressed TAF12.

Nevertheless, knockdown of TAF12 is not sufficient to reverse the Caco-H phenotype. A possible explanation is that cells have acquired nonreversible changes during the EMT. Alternatively, and as suggested by others (31), a transient modification in E-cadherin levels could be insufficient to produce a reversion. A third possibility is that TAF12 specifically directs the transcription of only a subset of genes implicated in EMT. The observations of this study support the third explanation because no change in expression of several other genes tested was observed, most notably of *vimentin* expression, a characteristic EMT marker.

We have examined several colorectal cell lines and observed that some have partial EMT characteristics, such as repression of *E-cadherin* and/or up-regulation of *vimentin* at different degrees. Interestingly, the SW620 cell line, which in our hands showed both the more repressed E-cadherin and enhanced TAF12 and vimentin, has been established from a lymph node metastasis, has EMT characteristics, and is considered as a model for studying molecular events in the late stages of colon cancer (32). An appealing hypothesis is that EMT is a key event in colorectal tumor progression. Indeed, the transition from early adenoma represented by the Caco-2 cells to the late adenoma with metastatic properties such as SW620 cells could be mediated by different degrees of EMT defined by their content in E-cadherin and vimentin. Further work in cell lines and tumor samples is needed to show the dispensable presence of EMT in tumor progression as well as a biological relevance of TAF12 in EMT and cancer.

It has been shown that loss of one central TAF can affect the overall TFIID structure, thereby inducing degradation of other TAFs and further leading to the impediment of transcription (33). Specifically, the reduction of TAF12 by RNA interference in *Drosophila* Schneider cells results in a disorganization of TFIID (34). The results of our studies using the TAF12 siRNA confirm a reduction in several TAFs. Nevertheless, our data suggest a regulatory role of TAF12 for specific gene (group) regulation, which can influence particular cell properties, such as cell migration. In perfect agreement with this, recent studies show that, in the absence of TAFs, single cells are capable of fulfilling transcription but respond inappropriately (33). Future studies will be necessary to reveal the potential role of other TFIID members in regulating *E-cadherin* expression. This may lead to the discovery of new strategies aimed at uncoupling the RAS mutation from tumor development and progression.

Materials and Methods

Propagation and Treatment of Cell Lines

American Type Culture Collection cell lines as well as RAS clones were cultured in DMEM supplemented with 10% fetal bovine serum (FBS), antibiotics, and nonessential amino acids, all from Invitrogen Corp. The HKE3 cell line was described elsewhere (5). Cell lines were regularly passaged. All experiments were done at 80% confluence, unless differently stated. RAS mutations have been verified by sequencing. For MEK inhibition, cells were grown in 10% or 0.5% FBS for 24 h before inhibitor or DMSO addition (40 μmol/L UO126; Alexis Biochemicals). Inhibitor was incubated for 15 h, replaced by fresh, and incubated for an additional 5 h.

siRNA Transfection

Cells were transfected with human TAF12 individual siGENOME ON-TARGET duplex (D-012149-03), ETS1 ON-TARGETplus SMART pool composed of four different duplexes (L-003887-00), or the siCONTROL RISC-free siRNA (D-001210-03; Dharmacon) as described in the text by the calcium phosphate method done based on a previously published protocol (35). For one well of a 12-well plate, 40 μL of a solution containing 64 pmol of duplex siRNA and 0.25 mol/L $CaCl_2$ were mixed to 40 μL of 2× BES-buffered solution, incubated for 25 min at room temperature, and added to the cells in a total medium volume of 800 μL. Eight hours after transfection, cells were washed twice with medium and further incubated for the required period.

Protein Extraction and Western Blotting

Nuclear and cytoplasmic extracts were prepared following the protocol described elsewhere (36). Buffers were supplemented with protease and phosphatase inhibitors before use. Whole-cell lysates were prepared as described (37). Protein concentrations were determined by the method of Bradford (Bio-Rad protein assay). Nuclear (20 μg) and total extracts (40 μg) were subjected to SDS-PAGE and transferred to a nitrocellulose membrane (Pall Corp.). Immunoblotting was carried out using the following antibodies: anti-β-actin (Abcam); anti-phosphorylated ERK, anti-ETS1, anti-HRAS, anti-KRAS, anti-SAP1a, and anti-vimentin (Santa Cruz Biotechnology); anti-phosphorylated ELK1 (Cell Signaling Technology, Inc.); and anti-TAF4 (32TA; ref. 20), anti-TAF12 (22TA; ref. 38), anti-TAF4b (21), anti-TAF7 (19TA; ref. 39), anti-TAF10 (6TA) and anti-TBP antibody (2C1; ref. 40), and peroxidase-conjugated anti-mouse/rabbit IgG (Jackson ImmunoResearch Laboratories). Signal was obtained with the enhanced chemiluminescence plus Western blotting detection system (Amersham Biosciences) after exposure to Kodak Super RX film. Values were measured using the ImageQuant software (Amersham Biosciences). All the experiments were repeated at least thrice and representative images are shown.

RNA Extraction and Reverse Transcription

Total RNA isolation from cultured cells was done using the Trizol reagent (Invitrogen). Reverse transcription was carried out from 3.0 μg of purified RNA using the SuperScript reverse transcriptase (Invitrogen) and an oligo$(dT)_{15}$ in 20 μL following the manufacturer's instructions.

PCR and Real-time PCR

PCR was done in the presence of 1 to 3 μL of a 1:7 dilution of the reverse transcription reaction using the TaqDNA polymerase (Invitrogen) in a total volume of 25 μL containing 2.5 mmol/L $MgCl^{2+}$, 10 pmol of each primer, and 0.2 mmol/L deoxynucleoside triphosphate. Products were separated on 1.5% agarose gels containing ethidium bromide and quantified by digital imaging (ImageQuant, Molecular Dynamics). Results were confirmed from three independent experiments. Primers used for PCR were the following (5′ to 3′): glyceraldehyde-3-phosphate dehydrogenase (GAPDH), GAAGGTGAAGGTCGGAGT (forward) and CATGGGTGGAATCATATTGGAA (reverse); TAF12, CAGCCCTAATCAACCTCTCC (forward) and GCTAAGACGACCTCCTGCC (reverse); E-cadherin, CGACCCAACCCAAGAATCTA (forward) and GCTGGCTCAAGTCAAAGTCC (reverse); TBP, CACGAACCACGGCACTGATT (forward) and TTTTCTTGCTGCCAGTCTGGAC (reverse). Primers corresponding to integrin α6 receptor and vimentin are described in ref. 7.

Real-time quantification was carried out in 96-well PCR plates using a Bio-Rad iCycler and the iQ5 Multicolor Real-Time PCR detection system (Bio-Rad). Cycling conditions included a denaturing step of 3 min at 95°C followed by 40 cycles at 95°C for 40 s and annealing/elongation at 62°C for 40 s. Each reaction (25 μL) contained 1× iQ SYBR Green Supermix (Bio-Rad) and 150 nmol/L of each primer. Each gene was tested in triplicate. Results were analyzed on the iCycler software. Each value was normalized to GAPDH and expressed relatively to a reference. Primers for *GAPDH* and *TAF12* amplification were the same than those used for regular PCR (see sequence above). For real-time amplification of *E-cadherin*, primers had the following sequence (5′ to 3′): CTTACTGCCCCCAGAGGAT (forward) and GCTGGCTCAAGTCAAAGTCC (reverse), whereas those used for ETS1 were the following: ATACCTCGGATTACTTCATTAGC (forward) and GGATGGAGCGTCTGATAGG (reverse).

Electrophoretic Mobility Shift Assay

Standard gel shift assays were done based on the protocol described in ref. 23. Briefly, 8 μg of nuclear extracts were incubated for 60 min at room temperature with ^{32}P-labeled double-stranded probe ([γ-^{32}P]ATP; Amersham Biosciences) in the presence of 1.5 μg of poly(deoxyinosinic-deoxycytidylic acid) (Sigma-Aldrich). Reaction was loaded onto native 6% polyacrylamide gel containing 0.25× TBE [10× TBE: 89 mmol/L Tris base, 89 mmol/L boric acid, 20 mmol/L EDTA (pH 8.0)]. Gel was prerunned for 30 min at 250 V, runned at 125 V for 2 h, dried for 1.5 h, and exposed for 12 h to a storage phosphor screen (Amersham Biosciences). Scanning was done with Storm 860 scanner (Amersham Biosciences) and values were measured using ImageQuant software. For competition, 1 μL of nonlabeled probe (100 molar fold excess of the labeled probe) was incubated with nuclear extracts for 30 min before addition of the labeled probe. For supershift experiments, 3 μL of antibody were preincubated with extracts 1 h before addition of the probe. For double-stranded probe preparation, oligonucleotides were mixed in equimolar amounts, heated, and allowed to cool for 16 h. Top strand sequences of oligos (Operon Biotechnologies) are shown below (5′ to 3′) with the protein-binding sites indicated in bold and mutations underlined. The AP-1 oligonucleotide was derived from ref. 41. Double-stranded oligos were blunt ended.

ETS1-3: GATCTCGAGCC**GGAA**GTTCGA
ETST12wt: GCGGTGCC**GGAA**GTAGTCGGG
ETST12mut: GCGGTGCC**A**GAAGTAGTCGGG

ChIP Assay

Cells were grown to 80% confluence in 100-mm dishes, cross-linked with 1% formaldehyde for 10 min at room temperature, collected in ice-cold PBS in the presence of phenylmethylsulfonyl fluoride (0.5 mmol/L), and resuspended in swelling buffer [25 mmol/L HEPES (pH 7.8), 1.5 mmol/L $MgCl_2$, 10 mmol/L KCl, 0.1% NP40, 1 mmol/L DTT, 0.5 mmol/L phenylmethylsulfonyl fluoride, 10 μg/mL aprotinin]. After homogenization for 10 times in a Dounce homogenizer, nuclei were resuspended in sonication buffer [50 mmol/L HEPES (pH 7.9), 140 mmol/L NaCl, 1 mmol/L EDTA, 1% Triton X-100, 0.1% sodium deoxycholate, 0.1% SDS, 0.5 mmol/L phenylmethylsulfonyl fluoride, 10 μg/mL aprotinin]. Chromatin was sheared in an average range of 500 to 1,000 bp by sonication in a water bath, with generation of high-power ultrasound (Bioruptor, Diagenode): 15 cycles of 30 s on, 30 s off (1 cycle/min) at maximum power. Protein A-Sepharose matrix CL-4B (Amersham Biosciences AB) used for immunoprecipitation was presaturated with salmon sperm DNA (Sigma-Aldrich) and rabbit serum. Chromatin was precleared in the presence of protein A matrix, salmon sperm DNA, and rabbit serum during 1 h at 4°C. Precleared chromatin was incubated overnight in rotation with 8 μg (Ets-1 and Elk-1 from Santa Cruz Biotechnology) or 4 μg (acetylated histone H3; Upstate) of antibodies. Immunoprecipitation with protein A was done for 2 h at 4°C. Matrix was washed twice (10 min per wash) with sonication buffer, twice with washing buffer A [50 mmol/L HEPES (pH 7.9), 500 mmol/L NaCl, 1 mmol/L EDTA, 1% Triton X-100, 0.1% sodium deoxycholate, 0.1% SDS, 0.5 mmol/L phenylmethylsulfonyl fluoride, 10 μg/mL aprotinin], twice with washing buffer B [20 mmol/L Tris (pH 8.0), 1 mmol/L EDTA, 250 mmol/L LiCl, 0.5% NP40, 0.5% sodium deoxycholate, 0.5 mmol/L phenylmethylsulfonyl fluoride, 10 μg/mL aprotinin], and twice with TE buffer. Elution was done with 400 μL elution buffer [50 mmol/L Tris (pH 8.0), 1 mmol/L EDTA, 1% SDS]. After decross-linking and treatment with proteinase K (10 mg/mL), phenol/chloroform DNA extraction was done, DNA was resuspended in 20 μL TE buffer, and 5 μL were analyzed by PCR. PCR was done as described above for 35 cycles and an annealing temperature of 62°C. Half of the PCR was analyzed on an 8% polyacrylamide gel stained with ethidium bromide.

Primers used for amplification of the TAF12 promoter ETS site were the following (5′-3′): GCGGTGCCGGAAGTAGTC (forward) and GGCAGCAGCGTCTATCTCC (reverse).

Transwell Assay of Cellular Migration and Cell Adhesion Assay

Twenty-four hours after transfection with siRNA, cells were trypsinized, washed thrice in medium supplemented with 1% FBS, and counted with a Z2 Coulter Counter (Beckman Coulter). Cells (1×10^4) were plated into the top chamber of 8-μm-pore Transwell filter (Corning) mounted in a 24-well dish containing medium with 10% FBS. Before use, filters were precoated for 10 h at 4°C with fibronectin (10 μg/mL; Sigma-Aldrich) and washed thrice. Cells were allowed to migrate in 5% CO_2 for 30 h at 37°C, fixed with methanol for 10 min at room temperature, and stained with 0.1% crystal violet. The underside of the filters was examined with a 40× objective of a light microscope and number of migrating cells was determined for 10 randomly selected fields. Data were obtained from two independent experiments, each repeated twice. For cell adhesion assay, 50 μL of cell suspension (4×10^5 cells/mL) were seeded onto fibronectin-coated 96-well dishes and allowed to adhere for 30 min at 37°C. After methanol fixation and crystal violet staining, cells were washed with water and dye was solubilized with 30% acetic acid. Attachment was quantified by measuring the absorbance at 600 nm. For this experiment, fibronectin was used at 20 μg/mL. Coating was followed by incubation in 1× PBS + 0.5% (w/v) bovine serum albumin [1× PBS: 0.14 mol/L NaCl, 0.0027 mol/L KCl, 0.01 mol/L phosphate buffer (pH 7.4)] and three washes using PBS + 0.1% bovine serum albumin. Data were obtained from two independent experiments each done six times. SD function was used for error bar generation.

Confocal Laser Scanning Microscopy and Immunohistochemistry

For confocal laser scanning microscopy, cells were grown on glass coverslips, fixed in 4% paraformaldehyde (10 min; room temperature), and permeabilized with 0.1% Triton X-100 for 10 min. Cells were blocked with 5% FBS (v/v) for 1 h and stained using rabbit anti-E-cadherin antibody diluted 1:100 and mouse anti-TAF12 antibody diluted 1:200 in 1× PBS containing 2% rabbit serum for 16 h at 4°C. Samples were washed and stained with Alexa Fluor 488–conjugated goat anti-mouse and Alexa Fluor 555–conjugated goat anti-rabbit secondary antibodies (1:300; Molecular Probes, Invitrogen) in 1× PBS containing 2% rabbit serum. After washing, nuclei were stained with Hoechst 33258 (Sigma-Aldrich) for 10 min and coverslips were mounted on glass slides in Gelvatol medium + DABCO, sealed with nail varnish, and viewed with a Leica TCS SPE confocal laser scanning microscope (Leica Lasertechnik). The objective lens used was 40×/1.15. The LAS AF software was used for image acquisition. For immunofluorescence experiments, cells were grown in 48-well plates (Greiner Bio One), treated as described above, and stained with an actin antibody (1:100 in PBS + 1% FBS) for 16 h at 4°C. Alexa Fluor 488–conjugated goat anti-mouse secondary antibody was used (1:400). Cells were visualized with a Nikon Eclipse TE200 inverted fluorescence/phase-contrast microscope equipped with a Sony charge-coupled device camera.

References

1. Fearon ER, Vogelstein B. A genetic model for colorectal tumorigenesis. Cell 1990;61:759–67.

2. Bos JL. ras oncogenes in human cancer: a review. Cancer Res 1989;49:4682–9.

3. Marshall CJ. Ras effectors. Curr Opin Cell Biol 1996;8:197–204.

4. Campbell SL, Khosravi-Far R, Rossman KL, Clark GJ, Der CJ. Increasing complexity of Ras signaling. Oncogene 1998;17:1395–413.

5. Shirasawa S, Furuse M, Yokoyama N, Sasazuki T. Altered growth of human colon cancer cell lines disrupted at activated Ki-ras. Science 1993;260:85–8.

6. Li W, Zhu T, Guan KL. Transformation potential of Ras isoforms correlates with activation of phosphatidylinositol 3-kinase but not ERK. J Biol Chem 2004; 279:37398–406.

7. Roberts ML, Drosopoulos KG, Vasileiou I, et al. Microarray analysis of the differential transformation mediated by Kirsten and Harvey Ras oncogenes in a human colorectal adenocarcinoma cell line. Int J Cancer 2006;118:616–27.

8. Huber MA, Kraut N, Beug H. Molecular requirements for epithelial-mesenchymal transition during tumor progression. Curr Opin Cell Biol 2005; 17:548–58.

9. Grunert S, Jechlinger M, Beug H. Diverse cellular and molecular mechanisms contribute to epithelial plasticity and metastasis. Nat Rev Mol Cell Biol 2003;4: 657–65.

10. Boyer-Guittaut M, Birsoy K, Potel C, et al. SUMO-1 modification of human transcription factor (TF) IID complex subunits: inhibition of TFIID promoter-binding activity through SUMO-1 modification of hsTAF5. J Biol Chem 2005; 280:9937–45.

11. Bell B, Scheer E, Tora L. Identification of hTAF(II)80δ links apoptotic signaling pathways to transcription factor TFIID function. Mol Cell 2001;8: 591–600.

12. Geles KG, Freiman RN, Liu WL, Zheng S, Voronina E, Tjian R. Cell-type-selective induction of c-jun by TAF4b directs ovarian-specific transcription networks. Proc Natl Acad Sci U S A 2006;103:2594–9.

13. Metzger D, Scheer E, Soldatov A, Tora L. Mammalian TAF(II)30 is required for cell cycle progression and specific cellular differentiation programmes. EMBO J 1999;18:4823–34.

14. Johnson SA, Mandavia N, Wang HD, Johnson DL. Transcriptional regulation of the TATA-binding protein by Ras cellular signaling. Mol Cell Biol 2000;20: 5000–9.

15. Foulds CE, Hawley DK. Analysis of the human TATA binding protein promoter and identification of an ets site critical for activity. Nucleic Acids Res 1997;25:2485–94.

16. Zhong S, Zhang C, Johnson DL. Epidermal growth factor enhances cellular TATA binding protein levels and induces RNA polymerase I- and III-dependent gene activity. Mol Cell Biol 2004;24:5119–29.

17. Johnson SA, Dubeau L, Kawalek M, et al. Increased expression of TATA-binding protein, the central transcription factor, can contribute to oncogenesis. Mol Cell Biol 2003;23:3043–51.

18. Gangloff YG, Romier C, Thuault S, Werten S, Davidson I. The histone fold is a key structural motif of transcription factor TFIID. Trends Biochem Sci 2001; 26:250–7.

19. Felinski EA, Quinn PG. The coactivator dTAF(II)110/hTAF(II)135 is sufficient to recruit a polymerase complex and activate basal transcription mediated by CREB. Proc Natl Acad Sci U S A 2001;98:13078–83.

20. Mengus G, May M, Carre L, Chambon P, Davidson I. Human TAF(II)135 potentiates transcriptional activation by the AF-2s of the retinoic acid, vitamin D3, and thyroid hormone receptors in mammalian cells. Genes Dev 1997;11: 1381–95.

21. Mengus G, Fadloun A, Kobi D, et al. TAF4 inactivation in embryonic fibroblasts activates TGFβ signalling and autocrine growth. EMBO J 2005;24: 2753–67.

22. Hamard PJ, bies-Tran R, Hauss C, Davidson I, Kedinger C, Chatton B. A functional interaction between ATF7 and TAF12 that is modulated by TAF4. Oncogene 2005;24:3472–83.

23. Fisher RJ, Mavrothalassitis G, Kondoh A, Papas TS. High-affinity DNA-protein interactions of the cellular ETS1 protein: the determination of the ETS binding motif. Oncogene 1991;6:2249–54.

24. Andreolas C, Kalogeropoulou M, Voulgari A, Pintzas A. Fra-1 regulates

vimentin during Ha-RAS-induced epithelial mesenchal transition in human colon carcinoma cells. Int J Cancer 2008;122:1745–56.

25. Seth A, Watson DK. ETS transcription factors and their emerging roles in human cancer. Eur J Cancer 2005;41:2462–78.

26. Zhong S, Fromm J, Johnson DL. TBP is differentially regulated by c-Jun N-terminal kinase 1 (JNK1) and JNK2 through Elk-1, controlling c-Jun expression and cell proliferation. Mol Cell Biol 2007;27:54–64.

27. Chastre E, Empereur S, Di GY, et al. Neoplastic progression of human and rat intestinal cell lines after transfer of the ras and polyoma middle T oncogenes. Gastroenterology 1993;105:1776–89.

28. Kurihara N, Reddy SV, Araki N, et al. Role of TAFII-17, a VDR binding protein, in the increased osteoclast formation in Paget's disease. J Bone Miner Res 2004;19:1154–64.

29. Palmer HG, Gonzalez-Sancho JM, Espada J, et al. Vitamin D(3) promotes the differentiation of colon carcinoma cells by the induction of E-cadherin and the inhibition of β-catenin signaling. J Cell Biol 2001;154:369–87.

30. Wong AS, Gumbiner BM. Adhesion-independent mechanism for suppression of tumor cell invasion by E-cadherin. J Cell Biol 2003;161:1191–203.

31. Andersen H, Mejlvang J, Mahmood S, et al. Immediate and delayed effects of E-cadherin inhibition on gene regulation and cell motility in human epidermoid carcinoma cells. Mol Cell Biol 2005;25:9138–50.

32. Hewitt RE, McMarlin A, Kleiner D, et al. Validation of a model of colon cancer progression. J Pathol 2000;192:446–54.

33. Marr MT, Isogai Y, Wright KJ, Tjian R. Coactivator cross-talk specifies transcriptional output. Genes Dev 2006;20:1458–69.

34. Wright KJ, Marr MT, Tjian R. TAF4 nucleates a core subcomplex of TFIID and mediates activated transcription from a TATA-less promoter. Proc Natl Acad Sci U S A 2006;103:12347–52.

35. Chen C, Okayama H. High-efficiency transformation of mammalian cells by plasmid DNA. Mol Cell Biol 1987;7:2745–52.

36. Schreiber E, Matthias P, Muller MM, Schaffner W. Rapid detection of octamer binding proteins with 'mini-extracts', prepared from a small number of cells. Nucleic Acids Res 1989;17:6419.

37. Drosopoulos KG, Roberts ML, Cermak L, et al. Transformation by oncogenic RAS sensitizes human colon cells to TRAIL-induced apoptosis by up-regulating death receptor 4 and death receptor 5 through a MEK-dependent pathway. J Biol Chem 2005;280:22856–67.

38. Mengus G, May M, Jacq X, et al. Cloning and characterization of hTAFII18, hTAFII20 and hTAFII28: three subunits of the human transcription factor TFIID. EMBO J 1995;14:1520–31.

39. Lavigne AC, Mengus G, May M, et al. Multiple interactions between hTAFII55 and other TFIID subunits. Requirements for the formation of stable ternary complexes between hTAFII55 and the TATA-binding protein. J Biol Chem 1996;271:19774–80.

40. Jacq X, Brou C, Lutz Y, Davidson I, Chambon P, Tora L. Human TAFII30 is present in a distinct TFIID complex and is required for transcriptional activation by the estrogen receptor. Cell 1994;79:107–17.

41. Rinehart-Kim J, Johnston M, Birrer M, Bos T. Alterations in the gene expression profile of MCF-7 breast tumor cells in response to c-Jun. Int J Cancer 2000;88:180–90.